Supporting Information for

Fault-Bound Valley Associated with the Rembrandt Basin on Mercury

Thomas R. Watters[1], Laurent G.J. Montési[2], Jürgen Oberst[3,4], Frank Preusker[3]

[1]Center for Earth and Planetary Studies, National Air and Space Museum, Smithsonian Institution, Washington, D.C. 20560-0315, USA

[2]Department of Geology, University of Maryland, College Park, MD 20742, USA

[3]German Aerospace Center, Institute of Planetary Research, D-12489 Berlin, Germany

[4]Moscow State University for Geodesy and Cartography (MIIGAiK), 105064 Moscow, Russia

Geophysical Research Letters

Contents of this file

Introduction

The supporting text, figure, and table provide further details on the elastic dislocation modeling using COULOMB to model two widely separated, opposite dipping thrust faults.

1. Elastic Dislocation Model

Deformation over thrust faults that propagates upward toward the surface are simulated using elastic dislocation modeling [*Lin and Stein, 2004*; *Toda et al*., 2005]. The magnitude and sense of slip is specified, and the stresses and material displacements are determined using the stress functions for an elastic half-space [*Okada*, 1992]. The fault surface is defined as a rectangular plane having a fault plane dip and vertical depth of faulting. An elastic half-space may not account for the effects of a weaker lower lithosphere, however, results obtained modeling deeply rooted terrestrial thrust faults [see Stein et al., 1994] suggest it is a reasonable approximation when its frictional stability is considered. A linear fault geometry is approximated by a single plane with a dip of 15°. A listric fault geometry is approximated by linear connecting fault segments with varying dips and lengths [*Watters*, 2004]. The dips of the fault segments are 40°, 30°, 20°, and 15°. Both fault geometries have a nearly flat (0.01°) final segment. Although the thrust faults are likely surface breaking, they are assumed to be blind. The upper tip of the near-surface thrust fault segment is fixed near the edge of the vergent side of the lobate scarp and the lower tip is fixed near the edge of the back-scarp slope, where the fault flattens (Figure S1). The length L, depth T, and dip θ of the fault segments are free parameters, as is the amount of displacement or slip D on the fault segments (Table S1, S2). An elastic modulus E of 80 GPa and Poisson's ratio **v** of 0.25 are assumed for Mercury's lithosphere. A full discussion of the sensitivity of the model parameters is given in Watters et al. [2002] and Watters [2004]. The flat segment (décollement) is assumed to extend for a distance at least several times the width of the scarps. The amount of slip on the flat segment were chosen to approximate the depths of the back-scarp troughs. The décollement may be regional in extent, but the predicted horizontal displacements are only significantly influenced if the terminus of the flat segment is near the edge of the back-scarp slope. In this case, a pronounced back-scarp syncline is predicted that is not observed in the topographic data. The amount of slip on the fault segments were selected to approximate the maximum relief of Enterprise Rupes and the Belgica Rupes--high-relief ridge.

References

Lin, J., R.S. Stein, Stress triggering in thrust and subduction earthquakes, and stress interaction between the southern San Andreas and nearby thrust and strike-slip faults, *J. Geophys. Res., 109*, B02303, doi:10.1029/2003JB002607, 2005.

Okada, Y., Internal deformation due to shear and tensile faults in a half-space, *Bull. Seism. Soc. Am.*, *82*, 1018-1040, 1992.

Stein, R. S., G. C. P. King, and J. Lin, Stress triggering of the 1994 M = 6.7 Northridge California, earthquake by its predecessors, *Science, 265*, 1432–1435, 1994.

Toda, S., R.S. Stein, K. Richards-Dinger, S. Bozkurt, Forecasting the evolution of seismicity in southern California: Animations built on earthquake stress transfer, *J. Geophys. Res., 110,* B05S16, doi:10.1029/2004JB003415, 2005.

Watters, T.R., Elastic dislocation modeling of wrinkle ridges on Mars, *Icarus*, *171*, 284-294, 2004.

Watters, T. R., R. A. Schultz, M. S. Robinson, and A. C. Cook (2002), The mechanical and thermal structure of Mercury's early lithosphere, *Geophys. Res. Letts., 29*, doi:10.1029/2001GL014308.

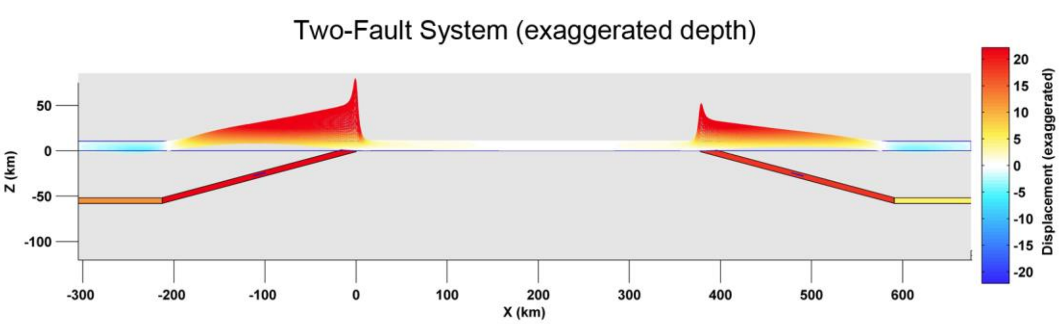

Figure S1. Cross-section showing a distorted grid resulting from displacements on two opposite dipping linear thrust faults. The two thrust faults are separated by a distance of ~400 km. The model parameters for the linear and listric fault geometries are given in Table S1 and S2. The vertical distance and displacement exaggeration is ~12:1.

Parameters for the Two-Fault System, Linear Model

Segment Number	*L*, km	θ	*T*, km	*D*, km
1	220.2	15°	60.0	4.050
2	573.0	0.01°	60.2	1.250
3	220.2	15°	60.0	6.500
4	573.0	0.01°	60.2	2.700

TABLE S1. Parameters for the two-fault linear COULOMB model. *L* is the along-dip length of the fault segment, θ is the dip of segment, *T* is the maximum depth of the segment and *D* is the specified slip on the segment. Segment numbers 1-2 are for the Belgica Rupes fault and segment numbers 3-4 are for the Enterprise Rupes fault.

Parameters for the Two-Fault System, Listric Model

Segment Number	*L*, km	θ	*T*, km	*D*, km
1	3.1	40°	6.0	3.025
2	4.0	30°	8.0	3.025
3	11.7	20°	12.0	3.025
4	185.4	15°	60.0	3.025
5	573.0	0.01°	60.2	1.000
6	3.1	40°	6.0	4.750
7	4.0	30°	8.0	4.750
8	11.7	20°	12.0	4.750
9	185.4	15°	60.0	4.750
10	573.0	0.01°	60.2	2.250

TABLE S2. Parameters for the two-fault listric COULOMB model. *L* is the along-dip length of the fault segment, θ is the dip of segment, *T* is the maximum depth of the segment and *D* is the specified slip on the segment. Segment numbers 1-5 are for the Belgica Rupes fault and segment numbers 6-10 are for the Enterprise Rupes fault.